Stem Cell Reports, Volume *11*

Supplemental Information

Generation of Progesterone-Responsive Endometrial Stromal Fibroblasts from Human Induced Pluripotent Stem Cells: Role of the WNT/CTNNB1 Pathway

Kaoru Miyazaki, Matthew T. Dyson, John S. Coon V, Yuichi Furukawa, Bahar D. Yilmaz, Tetsuo Maruyama, and Serdar E. Bulun

Supplemental Figure 1

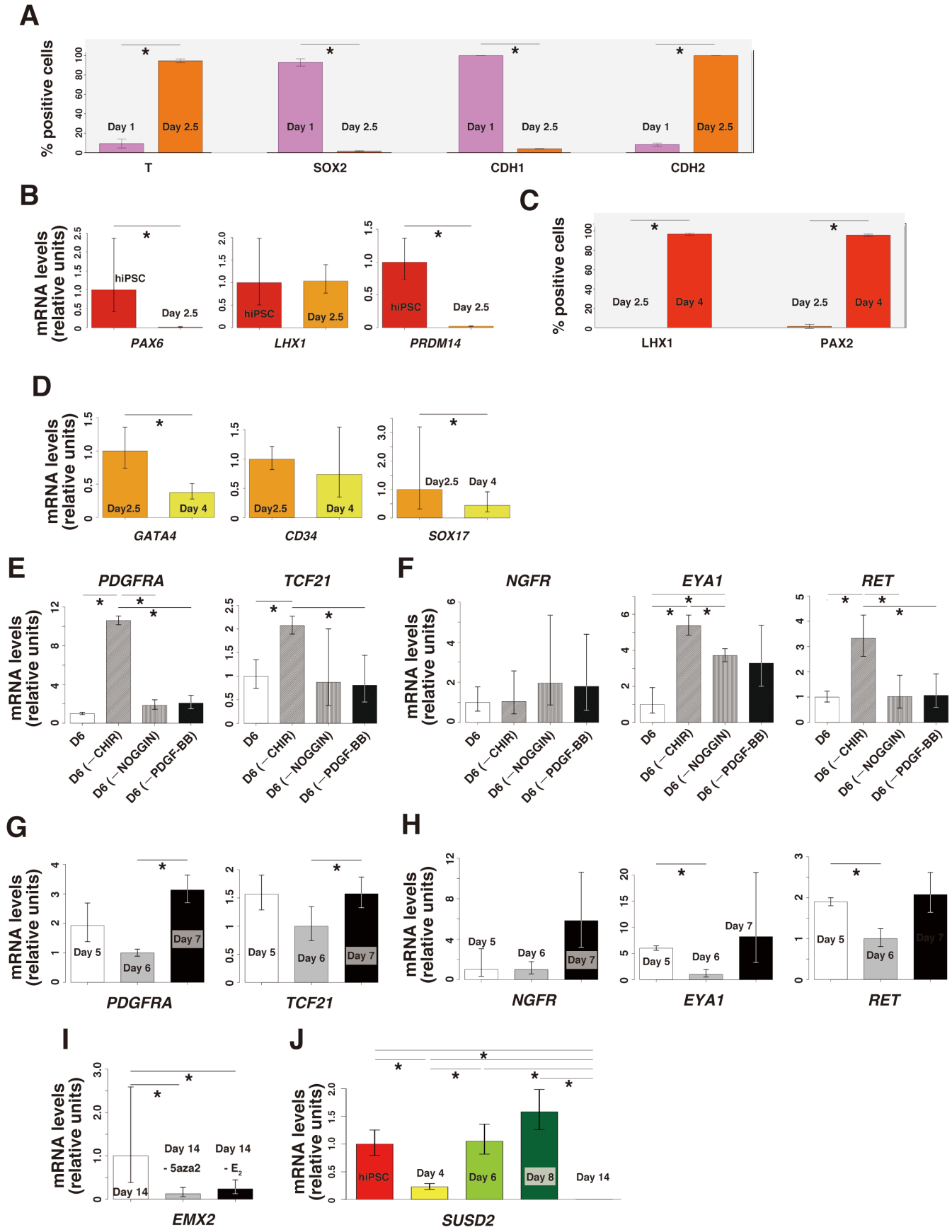

Supplemental Figure 2

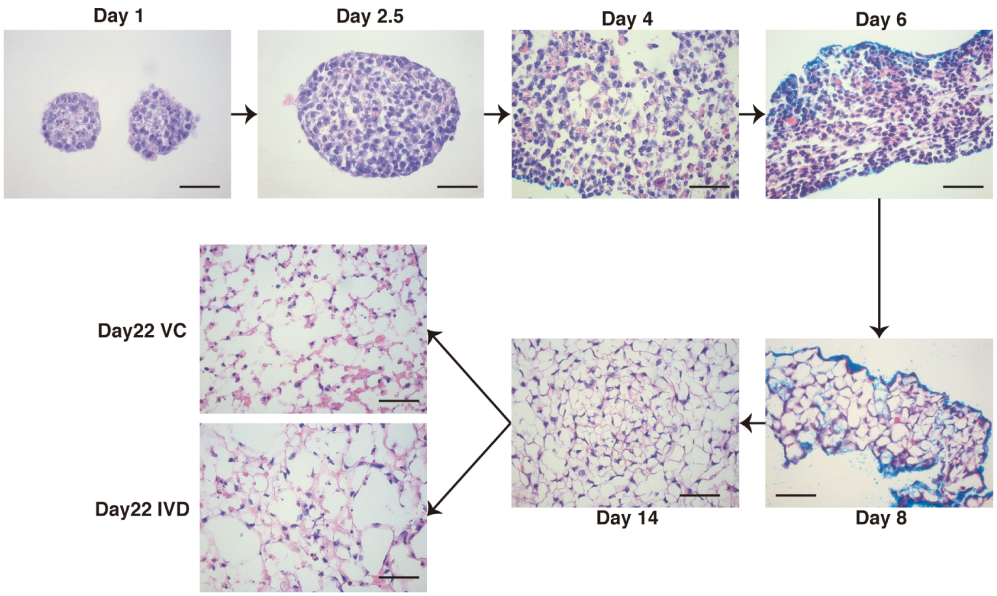

Supplemental Figure 3

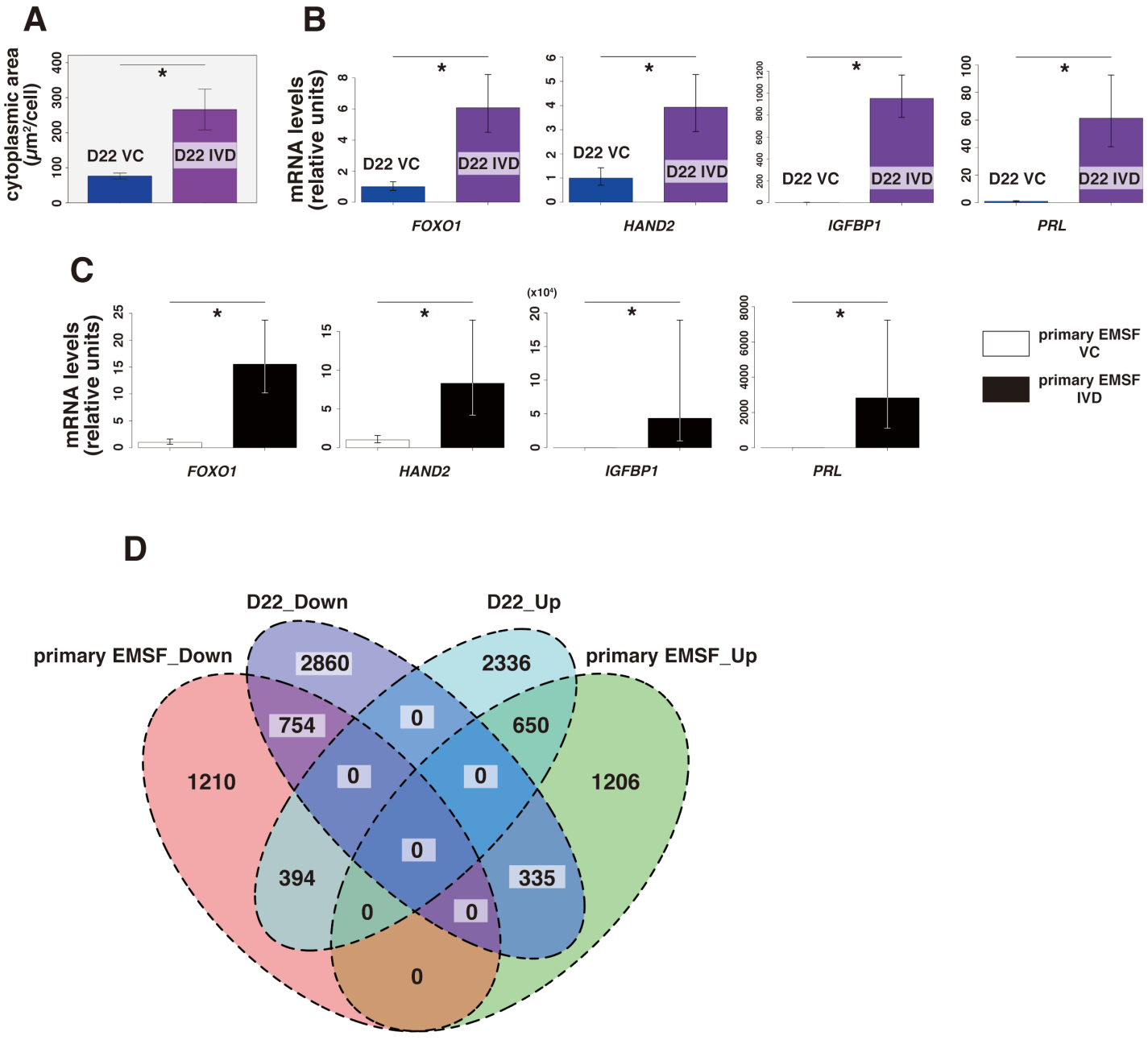

Supplemental Figure 4

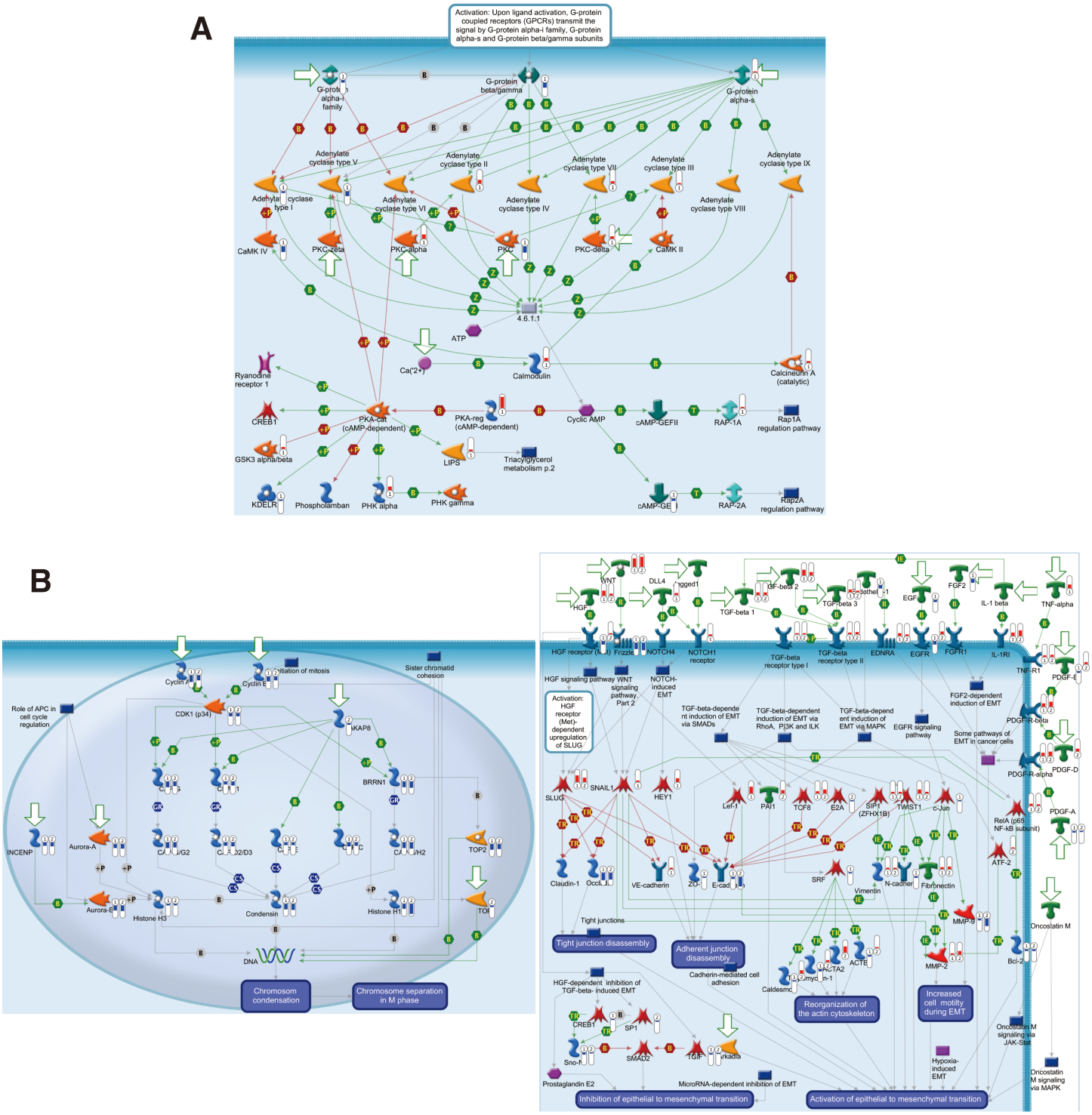

Supplemental Figure 5

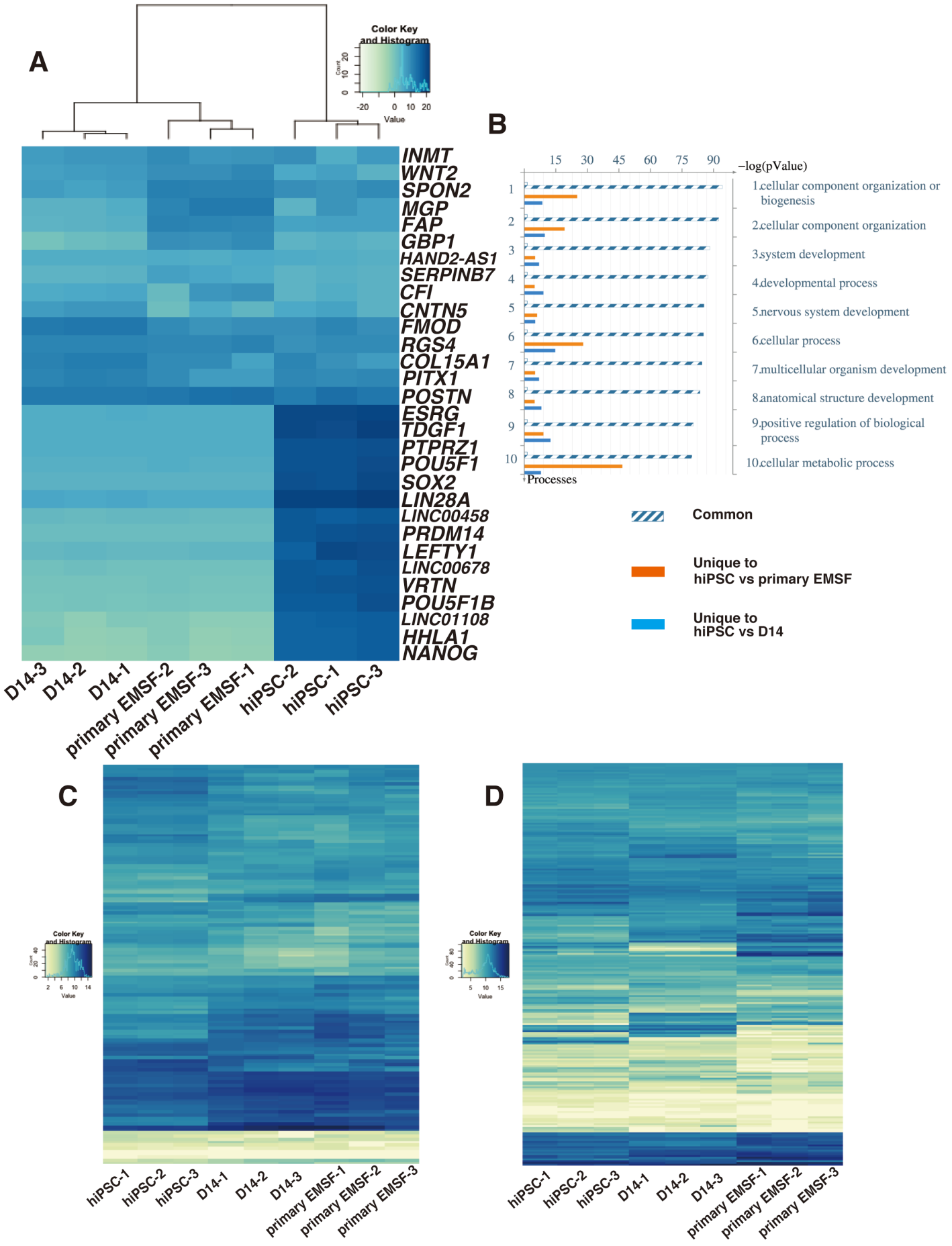

Supplemental Figure 6

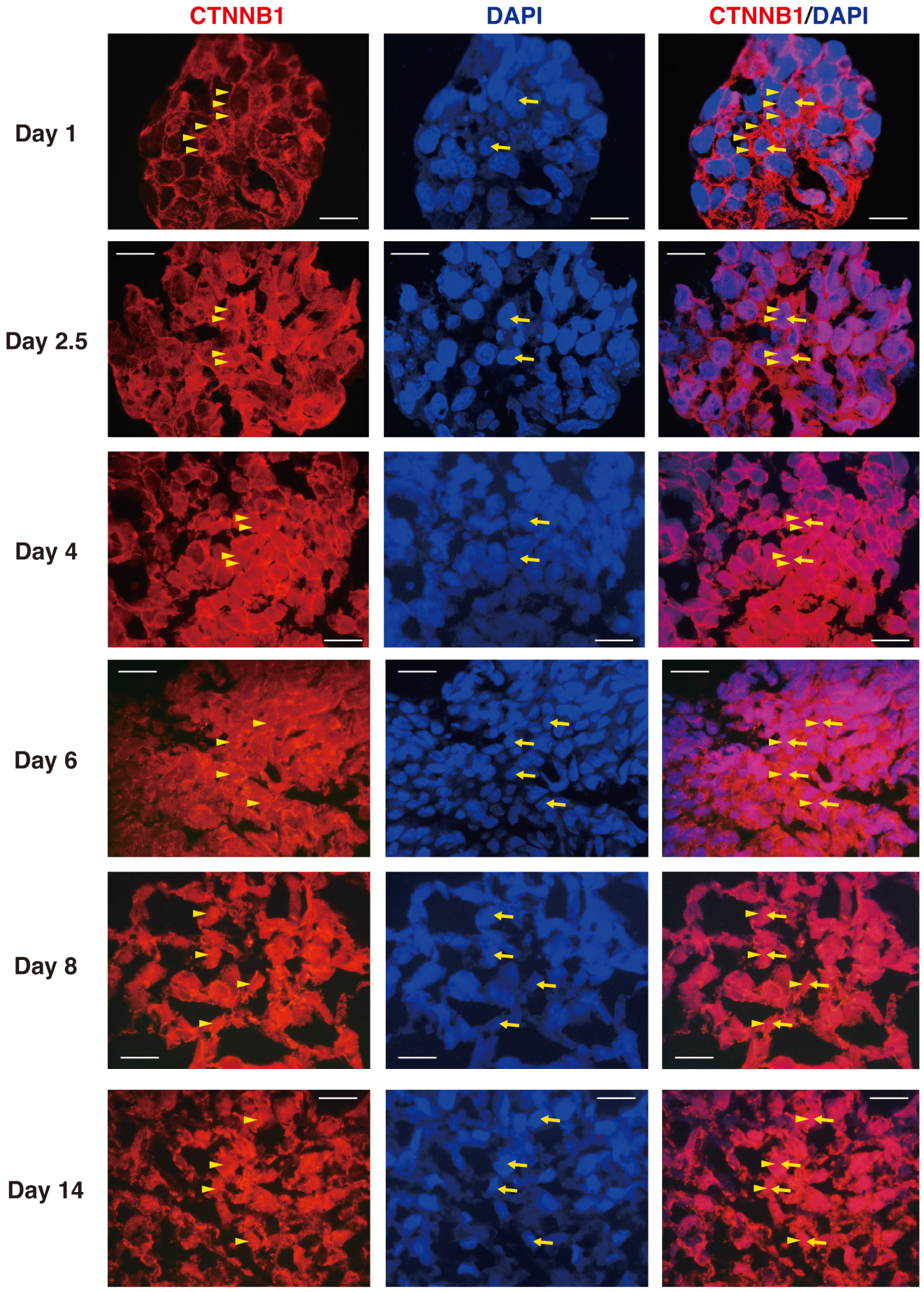

Supplementary Table 5: Primary antibodies used for flow cytometry

Antibody	**Company**	**Product number**	**Clone**	**Fluorochrome and isotype**	**Usage**
CD45	BD Biosciences	555485	HI30	APC-conjugated mouse IgG1	5 µl/1 × 10^6 cells
PDGFRA	BioLegend (San Diego, CA)	323506	16A1	PE-conjugated mouse IgG1	20 µl/1 × 10^6 cells
SUSD2	BioLegend	327406	W5C5	PE-conjugated mouse IgG1	5 µl/1 × 10^6 cells

Supplemental Table 6: List of primers used in qPCR

Target	Source	Product Id/Reference
ABRACL	Integrated DNA Technologies	Hs.PT.58.26763043
CD34	Integrated DNA Technologies	Hs.PT.56a.24708916
COL1A1	Thermo Fisher Scientific	Hs01076777_m1
EMX2	Integrated DNA Technologies	Hs.PT.58.39738222
EYA1	Integrated DNA Technologies	Hs.PT.58.39826997
FOXO1	Integrated DNA Technologies	Hs.PT.58.40005627
FN1	Integrated DNA Technologies	Hs.PT.58.40005963
GATA4	Thermo Fisher Scientific	Hs00171403_m1
HAND2	Integrated DNA Technologies	Hs.PT.58.4938123
HOXA10	Integrated DNA Technologies	Hs.PT.53a.20472403
HOXA11	Integrated DNA Technologies	Hs.PT.58.2064492
IGFBP	Integrated DNA Technologies	Hs.PT.58.3620731
ISL1	Integrated DNA Technologies	Hs.PT.58.2143768
KLF4	Integrated DNA Technologies	Hs.PT.58.45542593
LHX1	Integrated DNA Technologies	Hs.PT.58.3163761
NANOG	Integrated DNA Technologies	Hs.PT.58.21480849
NGFR	Integrated DNA Technologies	Hs.PT.58.4045496
NR5A1	Integrated DNA Technologies	Hs.PT.58.24264281
OSR1	Integrated DNA Technologies	Hs.PT.58.25056666
PAX2	Integrated DNA Technologies	Hs.PT.58.40853724
PAX6	Integrated DNA Technologies	Hs.PT.58.3002797
PDGFRA	Integrated DNA Technologies	Hs.PT.58.45699973
PGR	Thermo Fisher Scientific	Hs01556702_m1
PRDM14	Integrated DNA Technologies	Hs.PT.58.40121577
PRL	Integrated DNA Technologies	Hs.PT.58.3356588
RET	Integrated DNA Technologies	Hs.PT.58.4318912
SOX17	Integrated DNA Technologies	Hs.PT.58.24876513
SUSD2	Integrated DNA Technologies	Hs.PT.58.1294267
T	Integrated DNA Technologies	Hs.PT.58.1243965
TBP	Thermo Fisher Scientific	Hs99999910_m1

TBX6	Integrated DNA Technologies	Hs.PT.58.21333693
TCF21	Integrated DNA Technologies	Hs.PT.58.20883784
VIM	Integrated DNA Technologies	Hs.PT.58.38906895
ZFP42	Integrated DNA Technologies	Hs.PT.58.23001209

Supplemental Table 7: Primary antibodies used for immunostaining and Western blot

Antibody	Company	Product number	Clone	Appli-cation	Dilution	Retrieval (for IHC)	Incubation (for IHC)
ACTB	MilliporeSigma	A1978	AC-15	WB	1:10,000		
CDH1	Santa Cruz Biotechnology	sc-8426	G-10	IHC	1:50	ER1(20)= PH6	Leica Bond-Max Protocol F
CDH2	Thermo Fisher Scientific	33-3900	3B9	IHC	1:50	ER2(20)= PH9	Leica Bond-Max Protocol F
Type I collagen	SouthernBiotech (Birmingham, AL)	1310-01	Poly-clonal	IF, WB	1:30 (IF), 1:1,000 (WB)		
CTNNB1	BD Biosciences	610153	14	IF	1:100		
FOXO1	Cell Signaling Technology	14952	D7C1H	IHC, WB	1:100 (IHC), 1:1,000 (WB)	Ph6	Dako Autostainer plus 30/30
HOXA11	abcam (Cambridge, MA)	ab28699	Poly-clonal	IHC	1:200	ER1(20)= PH6	Leica Bond-Max Protocol F
HOXA11	Proteintech Group (Rosemont, IL)	55495-1-AP	Poly-clonal	WB	1:1,000		
ISL1	R&D Systems	AF1837	Poly-clonal	IF, WB	1:50 (IF), 1:200 (WB)		
LHX1	R&D Systems	MAB2725	320416	IHC, WB	1:200 (IHC), 1:1,000 (WB)	ER2(20)= PH9	Leica Bond-Max protocol F

NANOG	Thermo Fisher Scientific	PIPA1097	Poly-clonal	IHC, WB	1:200 (IHC), 1:1,000 (WB)	ER1(20)= PH6	Bond IHC Protocol F 15 min
PAX2	Thermo Fisher Scientific	71-6000	Poly-clonal	IHC, WB	1:150 (IHC), 1:1,000 (WB)	ER2(20)= PH9	Leica Bond-Max Protocol F H2O2 on the end
PDGFRA	Proteintech Group	60045-1-Ig	2C11B8	IHC, WB	1:100 (IHC), 1:1,000 (WB)	ER1(20)= Ph6	Leica Bond-Max protocol F
PGR	Agilent	M3569	PgR 636	IHC	1:100	ER1(20)	Leica Bond-Max Protocol PCF
PGR	Agilent	M356801-2	PgR 1294	WB	1:1,200		
PRLR	Cell Signaling Technology	M7018	D4A9	IHC, WB	1:200 (IHC), 1:100 (WB)	ER2(20)= PH9	Leica Bond-Max protocol PCF
SOX2	Cell Signaling Technology	2748	Poly-clonal	IHC, WB	1:100 (IHC), 1:1,000 (WB)	Ph6	Dako Autostainer plus Envision 30/15
T	Santa Cruz Biotechnology	sc-20109	Poly-clonal	IHC, WB	1:50 (IHC), 1:1,000 (WB)	ER1(20)= PH6	Leica Bond-Max Protocol F
VIM	Cell Signaling Technology	3932	Poly-clonal	WB	1:1,000		

Supplemental Figure 1. Assessment of cell-specific gene markers and cell morphology in EB during differentiation of hiPSC to EMSF. **(A)** Quantification of cells with positive immunofluorescence staining for T, SOX2, CDH1, and CDH2 in Day 1 and Day 2.5. Data represent mean ± SEM (N=3 independent experiments, *P<0.05, Student's t test for T and SOX2, Welch test for CDH1 and CDH2). **(B)** Quantitative RT-PCR comparing expression of *PAX6*, *LHX1*, and *PRDM14* in hiPSC and D2.5 EB. Genes are expressed in non-PS derivatives from EpiSCs. Error bars represent RQMin and RQMax (N=9 independent experiments, *P<0.05, Student's t test). **(C)** Quantification of cells with positive immunofluorescence staining for LHX1 and PAX2 in Day 2.5 and Day 4. Data represent mean ± SEM (N=3 independent experiments, *P<0.05, Student's t test for LHX1, Mann-Whitney test for PAX2). **(D-E)** Quantitative RT-PCR of coelomic epithelium (CE)-specific genes *PDGFRA* and *TCF21* **(D)** and non-CE derivative markers *NGFR*, *EYA*, and *RET* **(E)** in Day 6 EB. D6: D6 EB treated with CHIR, NOGGIN, and PDGF-BB; D6 (－CHIR): D6 EB treated with NOGGIN and PDGF-BB; D6 (－NOGGIN): D6 EB treated with CHIR and PDGF-BB; D6 (－PDGF-BB): D6 EB treated with CHIR and NOGGIN. Error bars represent RQMin and RQMax (N=3 independent experiments except for D6 (N=9 independent experiments), *P<0.05, Student's t test). **(F-G)** Quantitative RT-PCR of coelomic epithelium (CE)-specific genes *PDGFRA* and *TCF21* **(F)** and *NGFR*, *EYA*, and *RET* **(G)** in Day 5, 6, and 7 EB treated with CHIR, NOGGIN, and PDGF-BB. Error bars represent RQMin and RQMax (N=3 independent experiments except for D6 (N=9 independent experiments), *P<0.05, Student's t test). **(H)** Quantitative RT-PCR comparing expression of *GATA4*, *CD34*, and *SOX17* in D2.5 EB and D4 EB. Genes are expressed in non-IM derivatives from PS. Error bars represent RQMin and RQMax (N=9 independent experiments, *P<0.05, Student's t test). **(I)** Effect of withdrawal of 5aza2 or E_2 in mRNA expression level of *EMX2* in D14 EB. D14: D14 EB treated with 5aza2, CHIR, E_2, FGF9, and PDGF-BB; D14 - 5aza2: D14 EB treated with CHIR, E_2, FGF9, and PDGF-BB; D14 - E_2: D14 EB treated with 5aza2, CHIR, FGF9, and PDGF-BB for 6 days, between D8 and D14. Error bars represent RQMin and RQMax (N=3 independent experiments except for D14 (N=9 independent experiments), *P<0.05, Student's t test). **(J)** Quantitative RT-PCR comparing

expression of *SUSD2* in hiPSC, D4, D6, D8, and D14. Error bars represent RQMin and RQMax (N=9 independent experiments, *P<0.05, Student's t test).

Supplemental Figure 2. H&E staining of D1, D2.5, D4, D6, D8, D14, and D22 EB (IVD).

Supplemental Figure 3. In-vitro decidualization studies. **(A)** Quantification of cytoplasmic area in D22 VC and IVD. Data represent mean ± SEM (N=3 independent experiments, *P<0.05, Student's t test). **(B)** Quantitative RT-PCR of decidualization-specific genes *FOXO1*, *HAND2*, *IGFBP1*, and *PRL* in D22 VC and D22 IVD differentiated from clone 2 hiPSC. Error bars represent RQMin and RQMax (N=3 independent experiments, *P<0.05, Student's t test). **(C)** Quantitative RT-PCR of decidualization-specific genes *FOXO1*, *HAND2*, *IGFBP1*, and *PRL* in primary EMSF. Error bars represent RQMin and RQMax (N=3 independent experiments, *P<0.05, Student's t test). **(D)** Differentially expressed genes (DEGs) based on a comparison of RNA-seq data from D22 EB after IVD treatment and previous DNA microarray data from primary EMSF after IVD treatment (N=3 independent experiments, FDR adjusted p-value<0.05). The Venn diagrams show the total numbers of up- and downregulated genes identified in each comparison.

Supplemental Figure 4. Signaling pathways obtained from pathway enrichment analyses. **(A)** cAMP signaling pathway obtained from pathway analysis using MetaCore website based on DEGs in D22 IVD relative to vehicle control (N=3 independent experiments, FDR adjusted p-value<0.05). **(B)** Pathway maps obtained from pathway analysis using MetaCore based on DEGs in primary EMSF and D14 EB relative to hiPSC (N=3 independent experiments, FDR adjusted p-value<0.05). The pathway of chromosome condensation in prometaphase (left) and EMT pathway involving TGF and WNT/CTNNB1 signaling (right).

Supplemental Figure 5. Comparison of transcriptomes between hiPSC, hiPSC-derived EMSF, and primary EMSF. **(A)** Top 30 common DEGs in D14 and primary EMSF relative to hiPSC (N=3 independent experiments, FDR adjusted p-value<0.05). **(B)** Gene ontology

(GO) analysis using MetaCore (FDR < 0.05) performed on the same gene list used in **Figure 5D** (N=3 independent experiments, FDR adjusted p-value<0.05). The top 10 significantly enriched GO terms are shown with the -log of their FDR values on the x-axis. **(C)** Heatmap analysis comparing the expression of 133 cell cycle regulation genes in hiPSC, D14 EB, and primary EMSF (N=3 independent experiments). **(D)** Heatmap analysis comparing the expression of 232 genes that contributes to skeletal remodeling pathway and EMT pathway in hiPSC, D14 EB, and primary EMSF (N=3 independent experiments).

Supplemental Figure 6. Translocation of CTNNB1 during the differentiation of hiPSC. Single channel images of representative immunofluorescence for CTNNB1 in hiPSC, D2.5, D4, D6, D8, and D14 EB in Figure 7A were shown in this figure. Scale bars represent 20 μm. Yellow arrowheads indicate CTNNB1 staining. Yellow arrows indicate DAPI-positive cell nuclei.

Supplemental Table 1. List of pathways with FDR values obtained in the pathway enrichment analysis based on DEGs in D22 EB relative to vehicle control (top 200)

Supplemental Table 2. List of genes used in the heatmap analyses

Supplemental Table 3. List of pathways with FDR values obtained in the pathway enrichment analysis comparing DEGs in primary EMSF and D14 EB relative to hiPSC (top 200)

Supplemental Table 4. List of GO terms with FDR values obtained in the GO analysis comparing DEGs in primary EMSF and D14 EB relative to hiPSC (top 50)

Supplemental Table 5. List of antibodies used in the flow cytometry

Supplemental Table 6. List of primers used in qPCR

Supplemental Table 7. List of antibodies used in the immunostaining and western blots

SUPPLEMENTAL EXPERIMENTAL PROCEDURES

Differentiation

For all differentiation experiments, hiPSC grown on feeder layers of mitomycin C-treated MEFs were first dissociated by an enzymatic method with EDTA dissociation solution, and then incubated on gelatin-coated dishes for 30 min to remove MEFs. Then, the cells were dissociated into single cells by gentle pipetting after treatment with Accutase (Innovative Cell Technologies, San Diego, CA) for 20 min.

Cells were then plated at a density of 4.7 x 10^6 cells/well onto AggreWell400Ex (STEMCELL Technologies, Cambridge, MA) in hiPSC maintenance medium supplemented with 5 ng/ml recombinant human FGF2 and the ROCK inhibitor Y27632 10 mM (ApexBio Technology, Houston, TX) to form 4,700 embryoid bodies (EB) consisting of 1,000 cells. EB were harvested from AggreWell400Ex 24-32 hours after adding the hiPSC to the AggreWell400Ex, and plated at 2,350 EB/well in an ultra-low adherence 6-well plate (STEMCELL Technologies).

To induce PS and IM differentiation, a procedure described in Lam et al. (2014) was used. The media were changed to DMEM/F12 supplemented with 2 mM GlutaMAX, 100 IU/mL penicillin, 100 mg/mL streptomycin (Thermo Fisher Scientific), and CHIR (MedChemExpress, Monmouth Junction, NJ) for 36 hours to induce PS (D2.5 EB). EB were then treated with DMEM/F12 + 2 mM GlutaMAX + 1 x P/S + 100 ng/ml FGF2 + 1 mM retinoic acid (MilliporeSigma) for 36 hours to induce differentiation of IM (D4 EB).

For induction of CE, D4 EB were treated with basic differentiation medium (DMEM/F12 + 2.5% KnockOut Serum Replacement + 1 mM nonessential amino acids + 2 mM GlutaMAX + 0.55 mM 2-mercaptoethanol) supplemented with 3 μM CHIR, 5 ng/ml NOGGIN (PeproTech), and 10 ng/ml PDGF-BB (Thermo Fisher Scientific) for 2 days to produce CE (D6 EB). Controls were maintained in basic differentiation medium.

For induction of MD (D8 EB), the medium of D6 EB was changed to basic differentiation medium supplemented with 3 μM CHIR and 5 ng/ml NOGGIN for 2 days. To induce EMSF (D14 EB), D8 EB were treated with basic differentiation medium supplemented with 1 μM 5aza2 (MilliporeSigma), 3 μM CHIR, 10 ng/ml FGF-9 (R&D Systems, Minneapolis, MN), and 10 ng/ml PDGF-BB for 2 days, followed by the addition of 10^{-8}M E_2 (MilliporeSigma) for 4 days. Controls were maintained in basic differentiation medium.

To inhibit the canonical WNT/CTNNB1 pathway, D4, D6, and D8 EB were cultured without CHIR or treated with CTNNB1 inhibitors 5 μM IWP2 (R&D Systems, Minneapolis, MN) or 10 μM XAV939 (MilliporeSigma) in the presence of CHIR until D6, D8, and D14, respectively.

Flow cytometry analysis of D6 EB

D6 EB were dissociated into single cells by gentle pipetting after treatment with Accutase for 20 min. Dissociated D6 EB were resuspended at a concentration of 1×10^7 cells/ml in HBSS containing 2% KnockOut Serum Replacement (staining medium), and incubated with the PE-conjugated antibody against PDGFRA for 30 min at 4°C in the dark. The cells were then washed twice with cold staining medium, and fixed with 0.5% paraformaldehyde (Electron Microscopy Sciences, Hatfield, PA) in PBS overnight at 4°C in the dark, then washed with PBS, and resuspended in 3 μM 4’,6-diamidino-2-phenylindole (DAPI; Thermo Fisher Scientific) to label nonviable cells. Finally, the cells were subjected to flow cytometry analysis using BD FACSAria Cell Sorter (BD Biosciences (San Jose, CA)) to examine the percentage of PDGFRA+ cells. Forward scatter, side scatter, and DAPI gating excluded debris, doublets, and dead cells.

Isolation and culture of primary EMSF

Enzymes for tissue processing were obtained from MilliporeSigma. Cell culture media, trypsin, and supplements were from Thermo Fisher Scientific. Homogenous populations of primary EMSF were isolated from endometrial tissue as previously described (Ryan et al., 1994). Briefly, stroma and glandular fragments were dissected from adjacent tissue,

minced, and digested with collagenase and DNase at 37°C for 30 min. Samples were then treated with collagenase (MilliporeSigma), DNase (MilliporeSigma), protease (MilliporeSigma), and hyaluronidase (MilliporeSigma) at 37°C for an additional 30 min. Epithelial cells were eliminated by progressive filtration through sterile 70- and 20-μm sieves, and human EMSF were dispensed into 100-mm dishes for adherent growth and maintained in DMEM/F12 supplemented with 10% fetal bovine serum (FBS) (VWR International, Radnor, PA), 100 IU/mL penicillin, 100 mg/mL streptomycin, and 2.5 mg/mL amphotericin B (Thermo Fisher Scientific). Cells were maintained and grown in a humidified atmosphere with 5% CO_2 at 37°C, and medium was replenished every 48 h.

Isolation of SUSD2+ human eMSC

eMSC were isolated using flow cytometry according to the previously published protocol (Masuda et al., 2012). Briefly, dissociated EMSF were resuspended at a concentration of 2×10^6 cells/ml in HBSS containing 2% FBS (staining medium), and incubated with fluorescently labeled antibodies against CD45 and SUSD2 for 30 min at 4°C in the dark. The antibodies used are listed in Supplemental Table 5. The cells were then washed twice with cold staining medium and resuspended in 1 μg/ml propidium iodide (PI; MilliporeSigma) to label nonviable cells. Finally, the cells were subjected to fluorescent activated cell sorting (FACS) using BD FACSAria Cell Sorter to isolate SUSD2+ cells. Forward scatter, side scatter, and PI gating excluded erythrocytes, debris, doublets, and dead cells. Leukocytes (CD45+) were also excluded by electronic gating.

In vitro decidualization (IVD)

IVD regimens followed previous protocols with some modifications (Kim et al., 2007). Briefly, the medium was switched to phenol red-free DMEM/F12 media (Thermo Fisher Scientific) supplemented with 2% charcoal-dextran-stripped FBS and antibiotics after differentiation. Controls were maintained in this reduced medium, while IVD treatment consisted of 1 mM MPA (MilliporeSigma), 10^{-8} M E_2 (MilliporeSigma), and 0.3 mM cAMP (BIOLOG, Bremen Germany). Cells underwent 8-day IVD treatments.

RNA extraction, reverse transcription, and quantitative RT-PCR

Total RNAs were isolated from hiPSC, D2.5, D4, D6, D8, D14, D22 VC, D22 IVD EB, and primary EMSF using the RNeasy Mini Kit (Qiagen, Germantown, MD). The concentration of total RNA was measured by NanoDrop (Thermo Fisher Scientific). 266 ng of RNA was reverse-transcribed using the SUPERSCRIPT VILO (Thermo Fisher Scientific) to produce cDNA. For primers and probes, TaqMan gene expression assays (Thermo Fisher Scientific) or PrimeTime qPCR Assay (Integrated DNA Technologies, Coralville, IA) was used. RT-PCR reactions were run in duplicate using 3.8 ng cDNA, 500 nM primers, 250 nM probe, and TaqMan Universal PCR Master Mix (Thermo Fisher Scientific). Quantitative RT-PCR was performed using QuantStudio 12K Flex (Thermo Fisher Scientific). The cycling conditions were: 50°C for 2 min, 95°C for 10 min, and 40 cycles of 95°C for 15 s followed by 60°C for 1 min.

Expression levels were calculated by applying the comparative cycle threshold (Ct) method. Relative expression levels were normalized to the geometric mean of three housekeeping genes, RPL7, RPL15, and TBP, using ExpressionSuite Software Version 1.0.4 (Thermo Fisher Scientific). All qRT-PCR experiments were carried out with a non-template control. Primer information is provided in Supplemental Table 6.

Immunostaining of EB

EB were fixed with 4% paraformaldehyde in PBS for 30 min at RT, then washed three times in PBS. The EB were embedded in paraffin and sectioned at 5 µm. Richard-Allan Scientific HistoGel Specimen Processing Gel (Thermo Fisher Scientific) was used to encapsulate and retain D1, D2.5, and D4 EB during histological processing according to the manufacturer's protocol.

After deparaffinization and rehydration, the EB were then either stained with hematoxylin (MilliporeSigma) and eosin (VWR), or for individual proteins using primary antibodies and indirect immunostaining. See Supplemental Table 7 for antibody information. Immunofluorescence was performed for detection of type I collagen, CTNNB1, ISL1, and MME. Briefly, after antigen retrieval by heating in Target Retrieval Solution (Agilent, Santa Clara, CA), non-specific staining between the primary antibodies and the

tissue was blocked by incubating in blocking buffer (1% horse serum (VWR) in PBS) for 30 minutes at RT. The primary antibody was diluted in incubation buffer (1% FBS, 0.3% Triton X-100 (MilliporeSigma), and 0.01% sodium azide (MilliporeSigma) in PBS and applied to the sections. After incubation at 4°C overnight, the sections were washed with PBS and incubated with an anti-mouse Cy3 antibody (Jackson ImmunoResearch Laboratories, West Grove, PA) or anti-goat Alexa Fluor 488-conjugated antibody (Thermo Fisher Scientific) at RT for 1 hour. Nuclei were counterstained with DAPI (Thermo Fisher Scientific) at RT for 5 min.

For detection of other proteins, 3,3'-Diaminobenzidine (DAB) immunohistochemistry was performed using Dako Autostainer Plus (Agilent) or BOND-MAX Fully automated IHC and ISH (Leica Biosystems, Buffalo Grove, IL) with Bond Polymer Refine Detection (Leica Biosystems). Sections were mounted in ProLong Gold Antifade Mountant (Thermo Fisher Scientific) for immunofluorescence or Micromount (Leica Biosystems) for DAB immunohistochemistry and examined using an Automated Upright Microscope System for Life Science Research Leica DM5000 B (Leica Biosystems). Quantification was performed by counting three random fields at x100 magnification. Cytoplasmic volume was assessed on H&E staining and quantified as a two-dimensional area using ImageJ (Schneider et al., 2012). The real size of the image obtained at x100 magnification is 14,675.9 μm^2, and this corresponds to 7,990,272 pixels on ImageJ. Therefore, the cytoplasmic area was calculated using the following formula:

Cytoplasmic area (μm^2) = (number of pixels in cytoplasm) * 14,675.9 / 7,990,272

Cytoplasmic area per cell was obtained using cytoplasmic area and the cell number in the image to assess the average cytoplasmic volume of cells, and used for statistical analyses.

Preparation of protein and immunoblotting

Whole cell lysates were prepared by washing cells with PBS, followed by lifting and homogenizing the cells in RIPA buffer (50 mM Tris pH 7.6 (MilliporeSigma), 150 mM NaCl, 0.1% SDS, 0.5% sodium deoxycholate (MilliporeSigma), 1% IGEPAL CA-630

(MilliporeSigma)) supplemented with protease inhibitor cocktail (MilliporeSigma). Lysates were cleared by centrifugation at 14,000 x g for 10 min. Equal amounts of protein (20 µg) were resolved on NuPAGE Novex 4–12% bis-Tris Gels (Thermo Fisher Scientific). Transfer and membrane blocking were performed as previously described (Dyson et al., 2008). Incubation with primary antibodies (Supplemental Table 7) was performed at 4°C in 5% nonfat milk (Bio-Rad, Hercules, California) overnight. The membranes were then washed and incubated with the anti-mouse (Cell Signaling Technology, Danvers, MA), anti-rabbit (Cell Signaling Technology), or anti-goat (Santa Cruz Biotechnology, Dallas, TX) HRP-conjugated antibody for 1 h. Detection was performed using HyGLO Quick Spray Chemiluminescent HRP Antibody Detection Reagent (Denville Scientific, Holliston, MA), Luminata Crescendo HRP substrate (MilliporeSigma), or SuperSignal West Femto Maximum Sensitivity Substrate (Thermo Fisher Scientific). ImageJ software (National Institutes of Health, Bethesda, MD) was used to quantify immunoblot densitometry.

Enzyme-linked immunosorbent assay (ELISA)

IGFBP-1 levels in the conditioned media from D22 EB were assayed using ELISA kits from Alpha Diagnostic International (San Antonio, TX) according to the manufacturer's instruction. The minimum IGFBP-1 concentration detectable using this assay is 0.4 µg/L. Intra-assay coefficients of variation were 2.4–3.4% and inter-assay coefficients of variation were 5.0–7.4%. IGFBP-1 protein concentrations were normalized to genomic DNA content in each well. AllPrep DNA/RNA Mini Kit (Qiagen) was used to extract genomic DNA from EB. Genomic DNA content was measured using NanoDrop.

RNA-seq

For RNA-seq library preparation of hiPSC, D4, D6, D8, D14, D22 VC, D22 IVD, primary EMSF, and eMSC, DNA contaminants were digested with RapidOut DNA Removal Kit (Thermo Fisher Scientific). Total RNA quality was assessed using an Agilent Bioanalyzer 2100. RNA-seq libraries were constructed using KAPA Stranded RNA-Seq Kit with RiboErase (KAPA Biosystems, Wilmington, MA) following the manufacturer’s protocol. The ribosome RNAs were duplexed to DNA oligos and digested by RNase H treatment from

~500 ng DNAse-treated total RNA. Following purification, total RNA without ribosomal RNA was fragmented into small pieces using heat (94°C for 6 minutes) in the presence of Mg^{2+}. Under this condition, the average fragment length is 352 bp. Reverse transcriptase and random primers were used to copy the cleaved RNA fragments into first strand cDNA. The second strand cDNA was synthesized using DNA Polymerase I and dUTP in place of dTTP. These cDNA fragments then went through an A-tailing process, which adds dAMP to the 3′-ends of the cDNA library fragments, and adapter ligation, where double-stranded DNA adapters with 3′-dTMP overhangs are ligated to A-tailed library insert fragments. These products were then purified and enriched with 15 cycles of PCR to create the final cDNA library. The concentration of RNA libraries was measured by Qubit 3.0 Fluorometer (Thermo Fisher Scientific) and Qubit dsDNA Assay Kit (Thermo Fisher Scientific) following the manufacturer's protocol. The quality of RNA-seq library was measured by Agilent Bioanalyzer 2100. Three RNA samples from different experiments were used for constructing libraries for each stage.

cDNA libraries were sequenced as single-end, 75 base-length reads on an Illumina NextSeq 500 instrument (Illumina, San Diego, CA) with an average read count of 37 million reads per sample. Initial base calling and quality filtering of the RNA-seq reads generated with the Illumina analysis pipeline (fastQ format) were performed with the FastxToolkit (http://hannonlab.cshl.edu/fastx_toolkit/) and adapters trimmed by using CutAdapt (https://cutadapt.readthedocs.org/en/stable/). Reads were mapped (STAR v2.5.3a; https://github.com/alexdobin/STAR/archive/2.5.3a.tar.gz) to the reference genome (from Ensembl, v78; http://www.ensembl.org/index.html; Homo_sapiens.GRCh38.dna.primary_assembly.fa using Homo_sapiens.GRCh38.78.gtf as annotation).

Quantification and Statistical Analysis

Data analysis

For quantitative RT-PCR, relative quantification (RQ) (= $2^{-\Delta\Delta Ct}$) was obtained and a two-sample t-test was performed for statistical analysis using ExpressionSuite Software Version 1.0.4 (Thermo Fisher Scientific). Results are expressed as RQ with a range of

possible RQ values defined by the standard error (RQ min and max). For image analyses, immunoblot densitometry, and ELISA, distribution of each sample was assessed with the Shapiro-Wilk test. When the distributions of both samples were normal their dispersions were assessed with the Levene test. We compared homoscedastic samples using a two-sample t-test or for heteroscedastic samples, we used the Welch test. When at least either of the samples was not normally-distributed, they were compared using the Mann-Whitney test. IBM SPSS Statistics for Macintosh version 21.0 (IBM Corp., Armonk, NY) was used for these analyses. Results are expressed as means ± SEM.

For RNA-seq, differential expression P-values were calculated after normalizing expression values using DEseq2 (Love et al., 2014) (https://bioconductor.org/packages/release/bioc/html/DESeq2.html), an R package available through Bioconductor. R version 3.3.3 (R Development Core Team, 2014) was used for R-based analyses. P-values for expression differences between samples were then calculated in DEseq2 with a negative binomial distribution for gene expression. Finally, FDR (false discovery rate) for each P-value was calculated by DEseq2 using the Benjamini-Hochberg method.

PCA plot and hierarchical clustering with heatmap and dendrogram were generated using the R package “gplots.” Venn diagrams were generated using the R package “VennDiagram.”

For pathway enrichment analysis and GO analysis among different samples, MetaCore website (https://portal.genego.com) were used.

Reference

Dyson, M.T., Jones, J.K., Kowalewski, M.P., Manna, P.R., Alonso, M., Gottesman, M.E., and Stocco, D.M. (2008). Mitochondrial A-kinase anchoring protein 121 binds type II protein kinase A and enhances steroidogenic acute regulatory protein-mediated steroidogenesis in MA-10 mouse leydig tumor cells. Biology of reproduction *78*, 267-277.

Kim, J.J., Taylor, H.S., Lu, Z., Ladhani, O., Hastings, J.M., Jackson, K.S., Wu, Y., Guo, S.W., and Fazleabas, A.T. (2007). Altered expression of HOXA10 in endometriosis: potential role in decidualization. Molecular human reproduction *13*, 323-332.

Lam, A.Q., Freedman, B.S., Morizane, R., Lerou, P.H., Valerius, M.T., and Bonventre, J.V. (2014). Rapid and efficient differentiation of human pluripotent stem cells into intermediate mesoderm that forms tubules expressing kidney proximal tubular markers. Journal of the American Society of Nephrology : JASN *25*, 1211-1225.

Love, M.I., Huber, W., and Anders, S. (2014). Moderated estimation of fold change and dispersion for RNA-seq data with DESeq2. Genome biology *15*, 550.

Masuda, H., Anwar, S.S., Buhring, H.J., Rao, J.R., and Gargett, C.E. (2012). A novel marker of human endometrial mesenchymal stem-like cells. Cell transplantation *21*, 2201-2214.

R Development Core Team (2014). R: A language and environment for statistical computing (Vienna, Austria: R Foundation for Statistical Computing).

Ryan, I.P., Schriock, E.D., and Taylor, R.N. (1994). Isolation, characterization, and comparison of human endometrial and endometriosis cells in vitro. The Journal of clinical endocrinology and metabolism *78*, 642-649.

Schneider, C.A., Rasband, W.S., and Eliceiri, K.W. (2012). NIH Image to ImageJ: 25 years of image analysis. Nature methods *9*, 671-675.